

Content Based Retrieval of MRI Based on Brain Structure Changes in Alzheimer's Disease

Katarina Trojancanec, Ivan Kitanovski, Ivica Dimitrovski and Suzana Loshkovska
Department of Software Engineering, Faculty of Computer Science and Engineering, "Ss. Cyril and Methodius" University, "Rugjer Boshkovikj" 16, PO Box 393, 1000 Skopje, Macedonia

Keywords: CBIR, Alzheimer's Disease, VOI, Segmentation, Feature Extraction, Feature Selection, MRI, ADNI.

Abstract: The aim of the paper is to present Content Based Retrieval of MRI based on the brain structure changes characteristic for Alzheimer's Disease (AD). The approach used in this paper aims to improve the retrieval performance while using smaller number of features in comparison to the descriptor dimensionality generated by the traditional feature extraction techniques. The feature vector consists of the measurements of cortical and subcortical brain structures, including volumes of the brain structures and cortical thickness. Two main stages are required to obtain these features: segmentation and calculation of the quantitative measurements. The feature subset selection is additionally applied using Correlation-based Feature Selection (CFS) method. Euclidean distance is used as a similarity measurement. The retrieval performance is evaluated using MRIs provided by the Alzheimer's Disease Neuroimaging Initiative (ADNI). Experimental results show that the strategy used in this research outperforms the traditional one despite its simplicity and small number of features used for representation.

1 INTRODUCTION

Alzheimer's Disease (AD) is a progressive neurodegenerative disorder and the most common form of dementia for older adults. Its early diagnoses, monitoring the change in patient's condition or the progression of the disease, and identifying the patients who are most probable to ultimately develop AD are considered as very important challenges for physicians and researchers in this domain (Nho, 2012).

Magnetic Resonance Imaging (MRI) is found to be a powerful technique preferred to diagnosis of AD and its prodromal stage, Mild Cognitive

Impairment (MCI). It provides rich information needed for understanding and detecting disease pathology. This leads to enormously increased number of images stored in the medical databases that need to be efficiently organized, searched and analysed.

The systems that enable efficient retrieval on the basis of the image content are referred to as Content Based Image Retrieval (CBIR) systems. Being able to retrieve images from the database with similar Volume of Interest (VOI)/pathology/disease might be very useful in the clinical and research centres in two directions: (1) providing clinically relevant information to the physicians at right moment, thus supporting the diagnosis process and improving its quality and efficiency (Oliveira, 2007), and (2) for educational purposes (Rosset, 2004).

The searching capabilities of the CBIR systems in medical domain are still questionable and a big research challenge (Akgül, 2011). The reason is basically related to the specific nature of the medical images and subtle changes that need to be detected and taken into consideration. For example, limited resolution, intensity inhomogeneity, noise, and partial volume effects are characteristic for MRI and very often lead to geometrical inaccuracies

* Data used in preparation of this article were obtained from the Alzheimer's Disease Neuroimaging Initiative (ADNI) database (adni.loni.usc.edu). As such, the investigators within the ADNI contributed to the design and implementation of ADNI and/or provided data but did not participate in analysis or writing of this report. A complete listing of ADNI investigators can be found at:

http://adni.loni.usc.edu/wp-content/uploads/how_to_apply/ADNI_Acknowledgement_List.pdf

(Gerardin, 2009) that can directly affect the CBIR performance.

The main concern is to find a good representation of the image content by using techniques for feature extraction that will properly represent clinically relevant information and subsequently make the usage of medical CBIR systems more suitable, precise and clinically meaningful. To achieve this, the research is going towards its specialization in direction of (1) particular diseases, such as interstitial lung diseases (Depeursinge, 2011), AD (Akgül, 2009; Agarwal, 2010; Agarwal, 2011; Mizotin, 2012) etc., (2) body part such as brain (Akgül, 2009; Agarwal, 2010; Agarwal, 2011; Mizotin, 2012; Simonyan, 2013), lung (Depeursinge, 2011), or (3) the medical imaging techniques used for acquisition (e.g. Magnetic Resonance Imaging (MRI) (Simonyan, 2013), Computed Tomography (CT) (Moore, 2011), High-Resolution Computed Tomography (HRCT) (Depeursinge, 2011).

The focus of the paper is on CBIR of MRI applied to AD. Most of the current techniques in this domain focus on visual information extraction following the standard procedures of the traditional CBIR (Akgül, 2009; Agarwal, 2010; Agarwal, 2011; Mizotin, 2012). However, considering this approach in medical volumetric data context, the dimensionality and complexity become crucial problems.

To overcome this, we base the retrieval process on the structural changes in the human brain closely related to AD (Agarwal, 2011). Wide range of research has been performed to analyse their statistical dependence with respect to the disease (Gerardin, 2009; Lötjönen, 2011; Sabuncu, 2011; Nho, 2012). Some of them, including volume of the ventricular structures, hippocampus volume, amygdala volume or cortical thickness are used by the researchers for distinguishing or automatically labelling/classifying patients as AD, MCI, or healthy controls (Cuingnet, 2011; Gray, 2013), or to generate high-level semantic words used subsequently for the purpose of content based retrieval (Liu, 2013).

In this paper, the MRIs are represented by the measurements of brain structures, such as volumes of the separate structures and cortical thickness of the separate parts of the brain cortex. Two main stages are required: segmentation and calculation of quantitative measurements of the selected structures.

The feature selection is additionally applied to select the best discriminating feature subset. Experimental results show that this approach

outperforms the traditional one despite its simplicity and small number of features needed for representation.

The paper is organized as follows. Section 2 provides the state of the art. The experimental setup is explained in Section 3, while the experimental results obtained from the retrieval of MRIs applied to Alzheimer's Disease are given in Section 4. Section 5 provides concluding remarks and future directions.

2 STATE OF THE ART AND RELATED WORK

Several studies address CBIR in the context of AD (Akgül, 2009; Agarwal, 2010; Agarwal, 2011; Mizotin, 2012). Regarding the feature extraction used for CBIR in AD context, one usual direction is following the standard procedure used in the traditional CBIR through which image features are derived from the visual cues contained in the image.

For instance, intensity histograms, local binary pattern and gradient magnitude histograms are used to generate feature vector for the middle slice for subsequent usage in automated diagnosis of AD (Akgül, 2009). Discrete Cosine Transform (DCT), Daubechie's Wavelet Transform (DWT) and Local Binary Patterns (LBP) are used as descriptors (Agarwal, 2011). Again in this case, the descriptors are applied on 2D bases on a selected by radiologists subset of slices. Laguerre Circular Harmonic Functions expansions enabling capturing the local image patch structure directly are also used for feature extraction (Mizotin, 2012). The Bag-of-Visual-Words approach is then applied on a specific region (hippocampus). Slice by slice analysis is performed in this research.

The main disadvantage in the performed research in this area is that the feature extraction is performed only on one/several slice/s or slice by slice manner. This means excluding possibly significant information that might be extracted from the volumetric data. Another critical aspect is the dimensionality of the feature vector which can lead to a high computational complexity. For example, the size of each descriptor in (Akgül, 2009) is 256. Another example of the dimensionality of the traditional descriptors applied to volumes in the case of brain MRI includes: 13312 features for 3D Grey Level Co-occurrence Matrices, 1920 for 3D Wavelet Transforms, 9216 for Gabor Transforms and 11328 for 3D LBP per volume (Qian, 2011).

To overcome these disadvantages, the focus of this paper is to provide content based retrieval by using an alternative method for feature extraction. It is based on the structural changes considered as indicators for AD, including cortical thickness and volumes of the separate brain structures. While the traditional direction basically means extraction of the visual information itself, the alternative one utilizes the visual information to delineate the relevant brain structures (regarding AD in this case) on the bases of which the quantitative measurements are subsequently obtained. In the context of image retrieval, the first direction enables retrieval of images/Volumes of Interest (VOIs) with similar visual characteristics, while the second provides retrieval of images/VOIs with similar structural appearance with the query which in the context of AD is expected to lead to more relevant results.

To enable this, the pipeline that we propose to construct the feature vector includes these steps:

- Segmentation of the relevant brain structures/(VOIs)
- Calculating the measurements such as volume of the selected structures and cortical thickness
- Constructing the feature vector from the measurements obtained in the previous step

There is plenty of research based on making analysis of VOIs, relevant for detecting anatomical changes related to or imposed by AD. They usually include hippocampus, amygdala, ventricular structures, and brain cortex. For instance, multi-atlas segmentation framework used for segmentation of thalamus, caudate, putamen, pallidum, hippocampus and amygdala is proposed in (Lötjönen, 2010), and its improved version used for hippocampus segmentation described in (Lötjönen, 2011). Other methods for hippocampus extraction are proposed in (Chupin, 2009a; Chupin, 2009b). A method for cortical segmentation and parcellation is described in (Velayudhan, 2013). The anatomical segmentation of structural images of the human brain (83 regions) is depicted in (Heckemann, 2011).

Several software tools are also widely used by researchers in this domain for segmentation of different structures in the human brain, such as: FreeSurfer software package (FreeSurfer, 2013) used for cortical and subcortical segmentation (Moore, 2011), (Yuan, 2011), Brain Ventricular Quantification (BVQ) software (Accomazzi, 2009) for ventricular segmentation (Nestor, 2008), Statistical Parametric Mapping (SPM) software package for White Matter (WM), Grey Matter (GM),

and Cerebrospinal Fluid (CSF) segmentation (Nestor, 2008; Cataldo, 2013), Automatic Lateral Ventricle delineation (ALVIN) for lateral ventricle segmentation (Leonardo, 2011), as well as the FIRST tool as a part of FMRIB Software Library (FSL) (Leonardo, 2011). In this paper, the FreeSurfer software package is used, due to its powerful capabilities for segmentation and subsequent calculation of the measurements.

Additionally, with the aim to improve the retrieval results and increase the efficiency, we apply the feature selection step. As a result, we obtain better results in comparison to the reported results by the other authors while using very small number of features as a representation of the images.

The contributions of our research using this approach are: (1) key information extracted from the medical volume itself, (2) possibility to be adapted to reflect the change of the patient condition/disease progress (for future use), and (3) efficiency.

3 EXPERIMENTAL SETUP

3.1 Dataset

The images used for preparation of this research were obtained from the Alzheimer's Disease Neuroimaging Initiative (ADNI) database (adni.loni.usc.edu). The ADNI was launched in 2003 by the National Institute on Aging (NIA), the National Institute of Biomedical Imaging and Bioengineering (NIBIB), the Food and Drug Administration (FDA), private pharmaceutical companies, and non-profit organizations as a \$60 million, 5-year public-private partnership. The main goal of ADNI is to enable research on whether serial magnetic resonance imaging (MRI), positron emission tomography (PET), other biological markers, such as cerebrospinal fluid (CSF) markers, APOE status and full-genome genotyping via blood sample, as well as clinical and neuropsychological assessments can be combined to measure the progression of mild cognitive impairment (MCI) and Alzheimer's Disease (AD). Determination of sensitive and specific markers of very early AD progression is aimed to support the development of new treatments, to improve the process of monitoring treatments effectiveness, and to reduce the time and cost of clinical trials.

The Principal Investigator of this initiative is Michael W. Weiner, MD, VA Medical Center and University of California – San Francisco. ADNI is a valuable product resulting from the efforts of many

coinvestigators from a broad range of academic institutions and private corporations, and subjects have been recruited from over 50 sites across the U.S. and Canada. Initially, the goal of ADNI was to recruit 800 subjects. However, ADNI has been followed by ADNI-GO and ADNI-2, having recruited over 1500 adults, ages 55 to 90, to participate in the research. Cognitively normal individuals, adults with early or late MCI, and people with early AD can be distinguished in the dataset with different follow up duration of each group, specified in the protocols for ADNI-1, ADNI-2, and ADNI-GO. For up-to-date information, see <http://www.adni-info.org>.

3.2 Segmentation and Quantitative Measurements

The FreeSurfer software package pipeline version 5.1.0 was used to obtain the required measurements: volume of the brain structures and cortical thickness. The main methods from the FreeSurfer pipeline are summarized in Table 1 (Freesurfer Methods, 2014).

Due to the lack of neuroradiology expert, the quality control on the FreeSurfer output is not addressed in this research.

Table 1: Methods of the FreeSurfer pipeline.

Methods
Motion correction and averaging
Removal of non-brain tissue using a hybrid watershed/surface deformation procedure
Automated Talairach transformation
Segmentation of the subcortical white matter and deep grey matter volumetric structures
Intensity normalization
Tessellation of the grey matter white matter boundary
Automated topology correction
Surface deformation following intensity gradients
Registration to a spherical atlas
Parcellation of the cerebral cortex into units based on gyral and sulcal structure

3.3 Feature Representation

In this paper, the information extracted from the MRI volumetric data is represented on the basis of the quantitative measurements. After the segmentation has been conducted and the

measurements have been obtained, the feature vector is constructed. In this context, volume of the separate brain structures and cortical thickness of the separate cortical structures from the left and right hemisphere are used to compose the feature vector. It consists of 127 features.

Additionally, the feature subset selection method was applied with the aim to improve the retrieval performance and further reduce the feature vector dimensionality. For that purpose, Correlation-based Feature Selection (CFS) method was used. It evaluates subset of attributes taking into account the usefulness of individual features for predicting the class along the degree of intercorrelation among them (Hall, 2003).

4 EXPERIMENTAL RESULTS

The strategy used for this research was applied on two subsets of ADNI database: baseline images obtained using 3T scanners, and screening images obtained using 1.5T scanners. Both datasets have three classes of subjects: subjects with diagnosed AD, MCI, or normal controls (NL). The number of subjects in the dataset is given in Table 2.

Demographic information about the subjects such as gender and age is represented on fig. 1 (for the Baseline 3T subset) and fig. 2 (for the Screening 1.5T subset). However, this information does not have direct influence on the retrieval performance in the performed research, because it is based on the visual information only and subsequently obtained measurements.

Table 2: Subjects available for data sets.

Subset	Subjects available		
Baseline visits at 3T	Normal n = 47	MCI n = 71	AD n = 33
Screening visits at 1.5T	Normal n = 228	MCI n = 401	AD n = 188

In the case of MRIs of MCI subjects obtained by 1.5T scanners, five cases did not achieve successful FreeSurfer segmentation. These subjects were excluded from the retrieval process. All other subjects from the Baseline 3T MRI and Screening 1.5T MRI subset are considered.

Because the number of images in the subsets is not very large, leave-one-out strategy was performed. This means that each image was used as a query against all other images in the database. Euclidean distance was used as a similarity measurement.

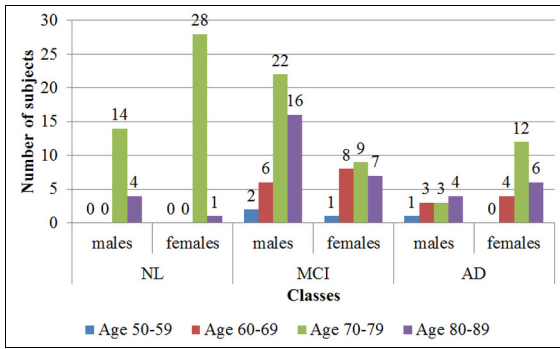


Figure 1: Demographic information such as gender and age per class (one of NL, MCI, AD) for the Baseline 3T subset. The horizontal axis denotes gender per each class, while the vertical one – the number of subjects. In each class, the number of subjects grouped by age range and gender is represented.

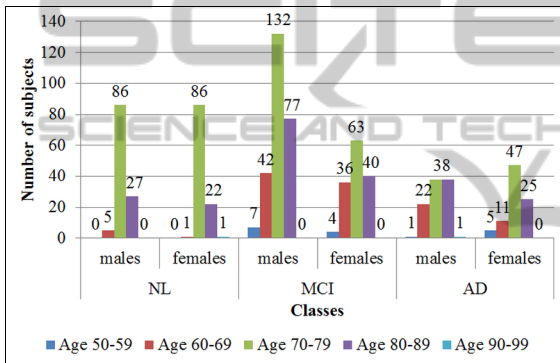


Figure 2: Demographic information such as gender and age per class (one of NL, MCI, AD) for the Screening 1.5T subset. The horizontal axis denotes gender per each class, while the vertical one – the number of subjects. In each class, the number of subjects grouped by age range and gender is represented.

To evaluate the retrieval performance, mean average precision (MAP) was used. The retrieved image is considered as relevant if it belongs to the same class as the query (AD, NL, MCI).

The retrieval performance is evaluated for both data sets in two cases:

- Considering only AD and NL subjects
- Considering all subjects (AD, NL, MCI)

The influence on the retrieval performance was also evaluated in the case when the whole feature vector (127 features) was used or the selected feature subset using CFS was applied.

4.1 Evaluation Performed on the 3T MRI Baseline Dataset

In this subsection, the results of the retrieval perfor-

mance evaluation conducted on the 3T MRI baseline dataset are given. Using the CFS method, the feature subset is selected. Table 3 summarizes the selected features in the case of two and three classes separately. Considering the selected feature subsets, it should be noted that most of these features are found to be valuable indicators for AD by the researchers including volume of the hippocampus, amygdala, lateral ventricles, entorhinal thickness etc. Thus, using these feature subsets in the subsequent retrieval process is very reasonable.

Table 4 and Table 5 summarize the results (on the bases of MAP) for each form of the feature vector (the whole, and the selected feature subset) considering the case with two and three classes for the Baseline 3T MRI dataset. When two classes are considered (AD and NL) the value of MAP is 0.53 if the images are represented with the whole feature vector. If the feature selection algorithm is applied, the MAP significantly increases to the value of 0.73. In this case, only 10 features are used. The case when all three classes are considered, the results are worse. Namely, the value of MAP without feature selection is 0.38. Applying the feature selection algorithm (leading to 13 features selected by the algorithm) improves the results to 0.47.

From the presented results it can be concluded that the feature subset selection significantly improves the results. From the other hand, the research conducted on the datasets in the case when MCI class is included, leads to decreased MAP. This can be explained by the nature of the MCI condition. Namely, it is usually transitional condition that very often develops to AD. Thus, it is very difficult to automatically make a distinction between this condition and AD or NL, and a big challenge in this domain. For example, it is recorded that the volume of hippocampus does not have as big discriminative power in distinguishing MCI and AD, as it has in distinguishing AD and NL (Gerardin, 2009). As a result, additional research is needed in this case, and is part of our future work.

To be able to compare the results to the results of the research performed on the same subset of ADNI dataset in (Mizotin, 2012) (Baseline 3T dataset with AD and NL classes), we also provide the curves of average precision at the first N (up to N=20) retrieved scans (fig. 3). According to the results reported in (Mizotin, 2012) for this subset, the best average precision reaches 0.74 (at N=1). In our case, we obtain better average precision of 0.78, at the same level. This means that the method for using measures of the brain structures used in this paper reaches even higher average precision at N=1 than

Table 3: Selected feature subsets for 3T MRI Baseline Dataset.

Classes included	NL, AD (10 features)	NL, AD, MCI (13 features)
Features	Left-Hippocampus	Left-Inf-Lat-Vent
	Right-Thalamus-Proper	Left-Hippocampus
	Right-Hippocampus	Left-Amygdala
	Right-Amygdala	Right-Lateral-Ventricle
	lh_entorhinal_thickness	Right-Inf-Lat-Vent
	lh_inferiortemporal_thickness	Right-Thalamus-Proper
	lh_parsorbitalis_thickness	Right-Hippocampus
	rh_entorhinal_thickness	Right-Amygdala
	rh_inferiorparietal_thickness	rh_entorhinal_thickness
	rh parahippocampal_thickness	rh parahippocampal_thickness
		lh_entorhinal_thickness
		lh_inferiortemporal_thickness
		lh_temporalpole_thickness

Table 4: Evaluation of the retrieval performance on the bases of MAP for 3T MRI Baseline Dataset (Classes: NL, AD).

Feature vector	MAP
All features (127 features)	0.53
After feature subset selection (10 features)	0.73

Table 5: Evaluation of the retrieval performance on the bases of MAP for 3T MRI Baseline Dataset (Classes: NL, AD, MCI).

Feature vector	MAP
All features (127 features)	0.38
After feature subset selection (13 features)	0.47

additionally provide curves of average precision at the first N (up to N=20) retrieved scans in the case when all three classes are considered (fig. 4).

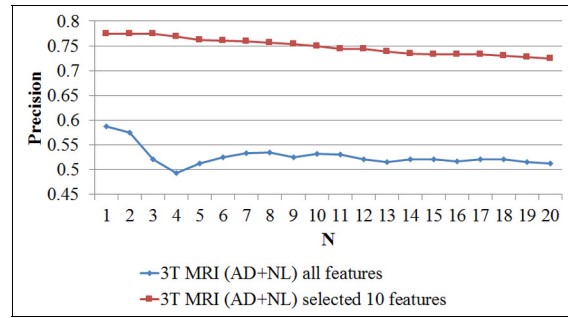


Figure 3: Precision at N (up to N=20) for the Baseline 3T subset of ADNI dataset (considered classes: AD and NL). N denotes the number of retrieved scans. The lower curve refers to the case when the all features are used. The upper curve applies to the case when only 10 features (obtained after the feature selection process) are used.

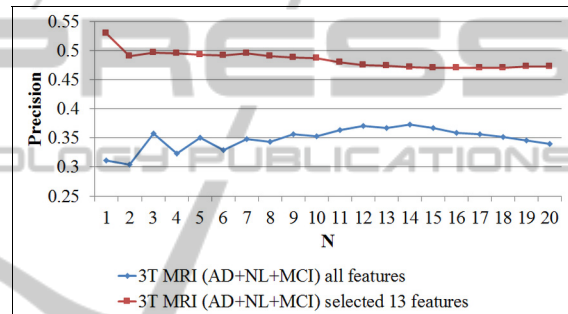


Figure 4: Precision at N (up to N=20) for the Baseline 3T subset of ADNI dataset (considered classes: AD, NL and MCI). N denotes the number of retrieved scans. The lower curve refers to the case when the all features are used. The upper curve applies to the case when only 13 features (selected by the feature selection algorithm) are used.

The results obtained from this research cannot be directly compared to the results obtained by the research about CBIR applied to Alzheimer’s Disease conducted by the other authors, because of the differences in the subsets used for evaluation.

4.2 Evaluation Performed on the 1.5T Screening MRI Dataset

The experimental results of the application of the proposed strategy to the dataset containing the screening visits at 1.5T are presented in this subsection. Table 6 contains the selected feature subset for the data set of 1.5T Screening MRIs in the case of two (NL and AD) and three classes (NL, AD and MCI). Similarly as in the case of 3T Baseline dataset, the most of the selected features are reported by the researchers as significant AD indicators.

Table 6: Selected feature subsets for 1.5T MRI Screening Dataset.

Classes included	NL, AD (17 features)	NL, AD, MCI (15 features)
Features	Left-Inf-Lat-Vent	Left-Inf-Lat-Vent
	Left-Hippocampus	Left-Hippocampus
	Left-Amygdala	Left-Amygdala
	Right-Putamen	Right-Hippocampus
	Right-Hippocampus	lh_bankssts_thickness
	Right-Amygdala	lh_entorhinal_thickness
	lh_bankssts_thickness	lh_fusiform_thickness
	lh_entorhinal_thickness	lh_inferiorparietal_thickness
	lh_inferiorparietal_thickness	lh_inferiortemporal_thickness
	lh_inferiortemporal_thickness	lh_middletemporal_thickness
	lh_middletemporal_thickness	lh parahippocampal_thickness
	lh parahippocampal_thickness	rh_entorhinal_thickness
	lh_rostralanteriorcingulate_thickness	rh_inferiortemporal_thickness
	rh_entorhinal_thickness	rh_middletemporal_thickness
	rh_inferiortemporal_thickness	rh parahippocampal_thickness
	rh_middletemporal_thickness	
rh parahippocampal_thickness		

The results (based on MAP) for the Screening 1.5T MRI dataset are given in Table 7 and Table 8 for both cases: the whole feature vector and the selected feature subset.

Table 7 summarizes the results when only two classes are considered, while the results in the case of three classes are depicted in Table 8. According to the obtained results, it should be noted that in the case when two classes are considered, the value of MAP is 0.51. By applying the feature selection algorithm, significantly increased value of MAP = 0.75 is obtained. In this case, a feature subset of 17 features was used to represent the images. In the

case when three classes are considered, the value of MAP is 0.37 if the whole feature vector is used. Applying the feature selection increases MAP to the value of 0.46.

Table 7: Evaluation of the retrieval performance on the bases of MAP for 1.5T MRI Screening Dataset (Classes: NL, AD).

Feature vector	MAP
All features (127 features)	0.51
After feature subset selection (17 features)	0.75

Table 8: Evaluation of the retrieval performance on the bases of MAP for 1.5T MRI Screening Dataset (Classes: NL, AD, MCI).

Feature vector	MAP
All features (127 features)	0.37
After feature subset selection (15 features)	0.46

We additionally provide curves of average precision at the first N (up to N=20) retrieved scans for the 1.5T Screening MRI dataset in the case when only NL and AD classes are considered (fig. 5) and in the case where all three classes are considered (fig. 6).

It should be emphasized that in all cases, the feature selection leads to significantly improved retrieval performance, while decreasing the retrieval process complexity. The reason is that including this step leads to reduction of irrelevant, redundant or possibly noisy data. In fact, only the most relevant and discriminative features are considered. From the perspective of the application domain of this research, it should be noticed that the selected features by the algorithm comply with the most

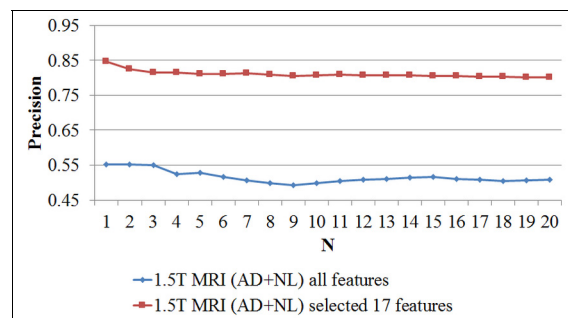


Figure 5: Precision at N (up to N=20) for the 1.5T Screening MRI subset of ADNI dataset (considering subjects with AD and NL). N denotes the number of retrieved scans. The lower curve refers to the case when all features are used. The upper curve applies to the case when the retrieval is based on 17 features only (obtained by using the feature selection algorithm).

significant AD markers listed in the literature (for example: hippocampus, amygdala, left and right lateral ventricles, entorhinal thickness etc.). This gives additional impact and makes this step even more meaningful.

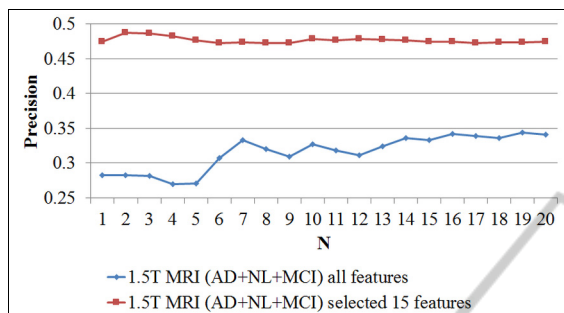


Figure 6: Precision at N (up to N=20) for the 1.5T Screening MRI subset of ADNI dataset (considering all three classes AD, NL and MCI). N denotes the number of retrieved scans. The lower curve refers to the case when all features are used. The upper curve applies to the case when the retrieval is based on 15 features only (obtained by using the feature selection algorithm).

In general, it can be concluded that the method used in this paper provides very promising results. It gives better retrieval results (on the bases of MAP) than the research conducted on the same dataset (3T Baseline MRI dataset) with very small number of features. This is very important result for the practical medical CBIR system. However, further investigation is needed in the case of inclusion of the MCI group, which is planned for our future work.

5 CONCLUSIONS

Content based retrieval strategy of MRI on the bases of the structural changes characteristic for Alzheimer's Disease was researched in the paper. The feature extraction was performed to reflect the brain structural changes. The feature vector consists of the volume of the brain structures, as well as the cortical thickness of the cortical regions. The feature subset selection using CFS method was also applied. The retrieval performance was evaluated on the Baseline 3T MRIs and Screening 1.5T MRIs from the ADNI database. The experiments were conducted in the case where only AD and NL subjects were taken into consideration, and in the case of all three categories, including MCI.

In this research, the results were significantly improved by involving feature selection procedure. Moreover, it should be emphasized that most of the

features selected by the feature evaluator are stressed in the literature as valuable indicators of AD. Comparing to the results obtained on the same subset (Baseline 3T MRI), the strategy used in this paper leads to better results with only 10 features. This dimensionality is quite smaller than the traditional feature vector length.

Considering the categories of subjects included in the research, the results of the retrieval process when the MCI group is excluded are significantly better. This is because of the nature of this condition and needs further research which is a part of our future work.

The approach used in this research is very beneficial. It provides information extraction using the required volumetric data and efficient information representation. The usage of the measurements such as volumes and thickness of the brain structures as a medical volume representation in the CBIR system, enables answering the questions of type "find all subjects that have similar anatomical structure to the query one" utilizing the visual information rather than "find all subjects that have similar visual properties to the query image/VOI" (which is characteristic for the traditional approach). This is very important regarding the application domain. Moreover, the approach used in this research gives a good opportunity to extend this work with the aim to address the progression of the disease.

ACKNOWLEDGEMENTS

Data collection and sharing for this project was funded by the Alzheimer's Disease Neuroimaging Initiative (ADNI) (National Institutes of Health Grant U01 AG024904) and DOD ADNI (Department of Defense award number W81XWH-12-2-0012). The National Institute on Aging, the National Institute of Biomedical Imaging and Bioengineering, and through generous contributions from the following: Alzheimer's Association; Alzheimer's Drug Discovery Foundation; Araclon Biotech; BioClinica, Inc.; Biogen Idec Inc.; Bristol-Myers Squibb Company; Eisai Inc.; Elan Pharmaceuticals, Inc.; Eli Lilly and Company; EuroImmun; F. Hoffmann-La Roche Ltd and its affiliated company Genentech, Inc.; Fujirebio; GE Healthcare; IXICO Ltd.; Janssen Alzheimer Immunotherapy Research & Development, LLC.; Johnson & Johnson Pharmaceutical Research & Development LLC.; Medpace, Inc.; Merck & Co., Inc.; Meso Scale Diagnostics, LLC.; NeuroRx

Research; Neurotrack Technologies; Novartis Pharmaceuticals Corporation; Pfizer Inc.; Piramal Imaging; Servier; Synarc Inc.; and Takeda Pharmaceutical Company are all funders of ADNI. ADNI clinical sites in Canada are supported and funded by the Canadian Institutes of Health Research. Private sector contributions are facilitated by the Foundation for the National Institutes of Health (www.fnih.org). The grantee organization is the Northern California Institute for Research and Education, and the study is coordinated by the Alzheimer's Disease Cooperative Study at the University of California, San Diego. ADNI data are disseminated by the Laboratory for Neuro Imaging at the University of Southern California.

Authors also acknowledge the support of the European Commission through the project MAESTRA - Learning from Massive, Incompletely annotated, and Structured Data (Grant number ICT-2013-612944).

REFERENCES

- Accomazzi V., Lazarowich R., Barlow, C. J., and Davey, B., 2009. U.S. Patent No. 7,596,267. Washington, DC: U.S. Patent and Trademark Office.
- Agarwal M., and Mostafa J., 2010 Image Retrieval for Alzheimer's Disease Detection. Medical Content-Based Retrieval for Clinical Decision Support. Springer Berlin Heidelberg. pp. 49-60.
- Agarwal, M., and Mostafa, J., 2011 Content-based image retrieval for Alzheimer's disease detection. In Content-Based Multimedia Indexing (CBMI), 2011 *9th International Workshop* on pp: 13-18.
- Akgül, C. B., Ünay, D., and Ekin, A., 2009. Automated diagnosis of Alzheimer's disease using image similarity and user feedback. In *Proceedings of the ACM International Conference on Image and Video Retrieval*, pp. 34.
- Akgül C. B., Rubin, D. L., Napel, S., Beaulieu, C. F., Greenspan, H., Acar, B., 2011. Content-based image retrieval in radiology: current status and future directions. *Journal of Digital Imaging*, vol. 24 no. 2, pp. 208-222.
- Cataldo R, Agrusti A, De Nunzio G, Carlà A, De Mitri I, Favetta M, Quarta M, Monno L, Rei L, Fiorina E; Alzheimer's Disease Neuroimaging Initiative, 2013. Generating a minimal set of templates for the hippocampal region in MR neuroimages. *Journal of Neuroimaging* 23, no. 3 pp. 473-483.
- Chupin M., Gérardin E., Cuingnet R., Boutet C, Lemieux L., Lehericy S., Benali H., Garnero L., and Colliot O., 2009a. Fully automatic hippocampus segmentation and classification in Alzheimer's disease and mild cognitive impairment applied on data from ADNI. *Hippocampus* 19, no. 6 pp: 579-587.
- Chupin A., Hammer A., Liu R.S., Colliot O., Burdett J., Bardin E., Duncan J.S., Garnero L., Lemieux L., 2009b. Automatic segmentation of the hippocampus and the amygdala driven by hybrid constraints: method and validation. *Neuroimage*. vol. 46, no. 3:749-761.
- Cuingnet R., Gérardin E., Tessieras J., Auzias G., Lehericy S., Habert M. O., Chupin M., Benali H., and Colliot O., 2011. Automatic classification of patients with Alzheimer's disease from structural MRI: a comparison of ten methods using the ADNI database. *Neuroimage* 56, no. 2 pp. 766-781.
- Depeursinge, A., Zrimec, T., Busayarat, S., Müller, H., 2011. 3D lung image retrieval using localized features. In *SPIE Medical Imaging, International Society for Optics and Photonics*, pp. 79632E-79632E.
- FreeSurfer, 2013. Available from: <<https://surfer.nmr.mgh.harvard.edu/>>. [25.08.2014]
- FreeSurfer methods, 2014. Available from: <<http://surfer.nmr.mgh.harvard.edu/fswiki/FreeSurferMethodsCitation>>. [25.08.2014].
- Gerardin E, Gaël C., Marie C., Rémi C., Béatrice D., Ho-Sung K., Marc N. et al., 2009. Multidimensional classification of hippocampal shape features discriminates Alzheimer's disease and mild cognitive impairment from normal aging. *Neuroimage* 47, no. 4, pp. 1476-1486.
- Gray, K. R., Aljabar, P., Heckemann, R. A., Hammers, A., and Rueckert, D., 2013. Random forest-based similarity measures for multi-modal classification of Alzheimer's disease. *NeuroImage*, 65, pp: 167-175.
- Hall, M. A., & Holmes, G., 2003. Benchmarking attribute selection techniques for discrete class data mining. *Knowledge and Data Engineering, IEEE Transactions on*, 15(6), 1437-1447.
- Heckemann R. A., Keihaninejad S, Aljabar P., Gray K. R., Nielsen C, Rueckert D., Hajnal J. V., and Hammers A, 2011. Automatic morphometry in Alzheimer's disease and mild cognitive impairment." *Neuroimage* 56, no. 4 p.: 024-2037.
- Leonardo I., 2011. Atrophy Measurement Biomarkers using Structural MRI for Alzheimer's Disease. *The 15th Int. Conference on Medical Image Computing and Computer Assisted Intervention (MICCAI)*.
- Liu, S., Cai, W., Song, Y., Pujol, S., Kikinis, R., & Feng, D., 2013. A Bag of Semantic Words Model for Medical Content-based Retrieval. In *MICCAI Workshop on Medical Content-Based Retrieval for Clinical Decision Support*.
- Lötjönen, J. M., Wolz, R., Koikkalainen, J. R., Thurfjell, L., Waldemar, G., Soininen, H., and Rueckert, D., 2010. Fast and robust multi-atlas segmentation of brain magnetic resonance images. *Neuroimage*, vol. 49, no. 3, 2352-2365.
- Lötjönen J., Robin W., Juha K., Valtteri J., Lennart T., Roger L., Gunhild W., Hilka S., and Daniel R., 2011. Fast and robust extraction of hippocampus from MR images for diagnostics of Alzheimer's disease. *Neuroimage* 56, no. 1, pp. 185-196.
- Mizotin, M., Benois-Pineau, J., Allard, M., and Catheline,

- G., 2012. Feature-based brain MRI retrieval for Alzheimer disease diagnosis. In *Image Processing (ICIP), 19th IEEE International Conference* on pp. 1241-1244.
- Moore D. W., Kovanlikaya I., Heier L. A., Raj A., Huang C., Chu K. W., and Relkin N. R., 2011 A pilot study of quantitative MRI measurements of ventricular volume and cortical atrophy for the differential diagnosis of normal pressure hydrocephalus. *Neurology research international* 2012.
- Nestor S. M., Raul R., Michael B., Matthew S., Vittorio A., Jennie L. W., Jennifer F., and Robert B., 2008. Ventricular enlargement as a possible measure of Alzheimer's disease progression validated using the Alzheimer's disease neuroimaging initiative database. *Brain* 131, no. 9 pp: 2443-2454.
- Nho, K., Risacher, L. S., Crane, P. K., DeCarli, C., Glymour, M.M., Habeck, C., Kim, S. et al., 2012. Voxel and surface-based topography of memory and executive deficits in mild cognitive impairment and Alzheimer's disease. *Brain imaging and behavior* vol. 6, no. 4 pp. 551-567.
- Oliveira, M. C., Cirne, W., and de Azevedo Marques, P. M., 2007. Towards applying content-based image retrieval in the clinical routine. *Future Generation Computer Systems*, vol. 23, no. 3, pp. 466-474.
- Qian, Y., Gao, X., Loomes, M., Comley, R., Barn, B., Hui, R., Tian, Z., 2011. Content-based re-trieval of 3D medical images. In *eTELEMED 2011, The Third International Conference on eHealth, Telemedicine, and Social Medicine*, pp. 7-12.
- Rosset A., Muller H., Martins M., Dfouni N., Vallée J.-P., Ratib O., 2004. Casimage project - a digital teaching files authoring environment, *Journal of Thoracic Imaging* vol. 19 no. 2, 1-6.
- Sabuncu, M. R., Desikan R. S., Sepulcre J., Yeo B. T. T, Liu H., Schmansky N. J., Reuter M. et al., 2011. The dynamics of cortical and hippocampal atrophy in Alzheimer disease. *Archives of neurology* 68, no. 8 pp: 1040-1048.
- Simonyan, K., Modat, M., Ourselin, S., Cash, D., Criminisi, A., Zisserman, 2013. A. Immediate ROI search for 3-d medical images. In: *Medical Content-Based Retrieval for Clinical Decision Support*, pp. 56-67, *Springer Berlin Heidelberg*.
- Velayudhan, L., Proitsi, P., Westman, E., Muehlboeck, J. S., Mecocci, P., Vellas, B., et al., 2013. Entorhinal cortex thickness predicts cognitive decline in Alzheimer's disease. *Journal of Alzheimer's Disease*, vol. 33, no. 3, pp. 755-766.
- Yuan, L., Wang, Y., Thompson, P. M., Narayan, V. A., and Ye, J., 2011. Multi-source feature learning for joint analysis of incomplete multiple heterogeneous neuroimaging data. *NeuroImage*, 61(3), pp: 622-632.